Effect of an Epidermal Growth Factor Receptor Inhibitor in Mouse Models of Lung Cancer

Ying Yan,[1] Yan Lu,[1] Min Wang,[1] Haris Vikis,[1] Ruisheng Yao,[1] Yian Wang,[1] Ronald A. Lubet,[2] and Ming You[1]

[1]Department of Surgery and The Alvin J. Siteman Cancer Center, Washington University School of Medicine, St. Louis, Missouri and [2]Chemoprevention Agent Development Research Group, National Cancer Institute, Bethesda, Maryland

Abstract

Gefitinib (Iressa, ZD1839) is a potent high-affinity competitive tyrosine kinase inhibitor aimed primarily at epidermal growth factor receptor (EGFR). Inhibitors in this class have recently been approved for clinical use in the treatment of advanced non–small cell lung cancer as monotherapy following failure of chemotherapy. We examined the efficacy of gefitinib on lung tumorigenesis in mouse models using both postinitiation and progression protocols. Gefitinib was given at a dose of 200 mg/kg body weight (i.g.) beginning either 2 or 12 weeks following carcinogen initiation. In the postinitiation protocol, gefitinib significantly inhibited both tumor multiplicity (~70%) and tumor load (~90%) in A/J or *p53*-mutant mice ($P < 0.0001$). Interestingly, gefitinib was also highly effective against lung carcinogenesis in the progression protocol when individual animals already have multiple preinvasive lesions in the lung. Gefitinib exhibited ~60% inhibition of tumor multiplicity and ~80% inhibition of tumor load when compared with control mice (both $P < 0.0001$). These data show that gefitinib is a potent chemopreventive agent in both wild-type and *p53*-mutant mice and that a delayed administration was still highly effective. Analyses of mutations in the *EGFR* and *K-ras* genes in lung tumors from either control or treatment groups showed no mutations in EGFR and consistent mutation in K-*ras*. Using an oligonucleotide array on control and gefitinib-treated lesions showed that gefitinib treatment failed to alter the activity or the expression level of EGFR. In contrast, gefitinib treatment significantly altered the expression of a series of genes involved in cell cycle, cell proliferation, cell transformation, angiogenesis, DNA synthesis, cell migration, immune responses, and apoptosis. Thus, gefitinib showed highly promising chemopreventive and chemotherapeutic activity in this mouse model of lung carcinogenesis. (Mol Cancer Res 2006;4(12):971–81)

Introduction

Lung cancer is currently the leading cause of cancer mortality in the United States (1). Although surgical resection can be curative for many early-stage cancers, the overall 5-year survival rate for all stages of lung cancer is only 15% (2). Thus, prevention is an important part of lung cancer control especially in high-risk populations, such as current smokers and former smokers. Chemoprevention is defined as the use of specific natural or synthetic chemical agents to reverse, suppress, prevent, or delay the carcinogenic process either by blocking the development of early lesions or by inhibiting the progression to invasive cancer.

Epidermal growth factor receptor (EGFR) is a promising target for anticancer therapy because it is activated in a wide variety of cancers. Gefitinib (Iressa, ZD1839), a competitive EGFR tyrosine kinase inhibitor, was selected from a variety of substituted 4-(3-chloroanilino)-quinazolines as the most effective in inhibiting tyrosine kinases activity (3). It is an anilinoquinazoline compound with the chemical name 4-quinazolinamine, *N*-(3-chloro-4-flurophenyl)-7-methoxy-6-[3-(4-morpholinyl)propoxy]. Several *in vitro* and *in vivo* studies have shown that gefitinib can inhibit the growth of cancer cells and suppress the growth of xenografts (4, 5). Small-molecule EGFR inhibitors have recently been approved for clinical use in the treatment of advanced non–small cell lung cancer (NSCLC) as monotherapy following failure of chemotherapy (6). In two phase II trials, the response rates to gefitinib ranged from 11.8% to 18.4% (7, 8). Interestingly, the likelihood of a clinical response to gefitinib is greatly increased in lung cancer when activating mutations in the tyrosine kinase domain of the EGFR were found (9, 10). A smaller percentage of advanced lung cancers without EGFR mutations as well as other cancers lacking EGFR mutations, including head and neck, colon, and breast, seem to respond to gefitinib (11).

Mouse models allow vigorous preclinical characterization of efficacy and determination of mechanisms that can support phase II/III human chemopreventive clinical trials (12-14). Although gefitinib induces clinical responses in a subset of treated lung cancer patients, it has not been tested as a cancer prevention agent. Using a protocol to assess its role in prevention and a protocol to assess its role in progression, we treated a cohort of mice that had been exposed to benzo(*a*)pyrene

Received 3/29/06; revised 9/21/06; accepted 10/5/06.
The costs of publication of this article were defrayed in part by the payment of page charges. This article must therefore be hereby marked advertisement in accordance with 18 U.S.C. Section 1734 solely to indicate this fact.
Note: Supplementary data for this article are available at Molecular Cancer Research Online (http://mcr.aacrjournals.org/).
Requests for reprints: Ming You, Department of Surgery and The Alvin J. Siteman Cancer Center, Washington University, Campus Box 8109, 660 South Euclid Avenue, St. Louis, MO 63110. Phone: 314-362-9294; Fax: 314-362-9366. E-mail: youm@wudosis.wustl.edu

doi:10.1158/1541-7786.MCR-06-0086

(BaP), a carcinogen that induces lung tumors in mice. Treatment with gefitinib resulted in a substantial tumor prevention effect as well as a potent effect on blocking tumor progression. We also analyzed mutations in EGFR and K-*ras* in the resulting mouse lung tumors. Finally, we used Affymetrix microarrays (Affymetrix, Santa Clara, CA) to define genes whose expression was altered when comparing lesions from control and gefitinib-treated groups.

Results

Chemopreventive Efficacy of Gefitinib on BaP-Induced Lung Tumorigenesis in A/J Mice

Before the chemoprevention experiment presented here, we did an 8-week toxicity assay with gefitinib (Fig. 1A). Of doses from 100 to 400 mg/kg body weight, we found that a dose of 200 mg/kg body weight did not cause mortality or significantly affect body weight. Thus, the daily dose used was 200 mg/kg for this study. The daily dose of gefitinib in humans is 250 to 500 mg.[3] Based on the updated Guidance for Industry: Estimating the Maximum Safe Starting Dose in Initial Clinical Trials for Therapeutics in Adult Healthy Volunteers, U.S. Department of Health and Human Services, Food and Drug Administration, Center for Drug Evaluation and Research,[4] the conversion factor is 12.3 for converting mouse dose in mg/kg to human equivalent dose in mg/kg. Assuming human body weight as 60 kg (as the guidance indicated), the mg/kg in human is 500 / 60 = 8.3 mg/kg. When we converted the dose we used in the study (200 mg/kg in mouse) by the factor of 12.3, the human equivalent dose is 200 / 12.3 = 16.3 mg/kg. It was just less than two times higher than the clinical dose in humans.

We began with the postinitiation protocol (Fig. 2A, *a*). Gefitinib treatments in either wild-type or $p53^{mut/wt}$ mice were started 2 weeks after exposure to BaP and terminated at 20 weeks after BaP. It was continued for a total of 18 weeks and caused no significant body weight loss at the dose of 200 mg/kg. However, some treated mice showed light alopecia especially at the region near the eyelid (Fig. 1B). All the mice developed lung tumors following exposure to the carcinogen. The administration of gefitinib showed potent preventive effects on BaP-induced lung tumorigenesis. Gefitinib significantly reduced tumor multiplicity by 62% and 75% in wild-type and $p53^{mut/wt}$ mice, respectively (Fig. 3A). On the total tumor load, which reflects both tumor multiplicity and tumor size, the treatment of gefitinib showed even more striking effects. Tumor load was decreased by 89% and 94% in wild-type and $p53^{mut/wt}$ mice, respectively (Fig. 3B). Interestingly, the tumor size was in the range of 0.6 to 2.0 mm (diameter) in ~80% of the animals in the control group. In contrast, the majority of the tumors (77%) found in the gefitinib-treated group were significantly smaller and in the range of 0.2 to 0.5 mm (diameter), although in the gefitinib-treated group all pulmonary lesions were hyperplasias or adenomas. These results indicate that gefitinib

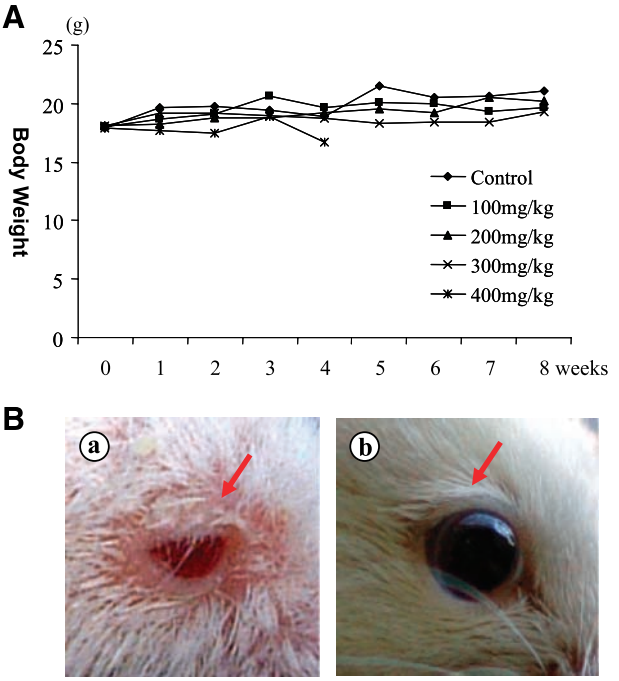

FIGURE 1. Preliminary toxicology of gefitinib in A/J mice. **A.** Preliminary toxicology bioassay. Five mice in each group were treated with different doses of gefitinib at control, 100 mg/kg, 200 mg/kg, 300 mg/kg, and 400 mg/kg body weight by gavage in 0.2 mL of 1% Tween 80 solution, five times per week, for 8 wk. The mice in 400 mg/kg group were terminated within first 4 wk because half of mice in this group died at the 4th week of the administration. **B.** Alopecia. Red arrow, during the 8 wk of gefitinib treatment, some mice showed light alopecia especially at the region near eyelid. **a,** gefitinib-treated mouse with alopecia near eyelid; **b,** normal mouse without gefitinib treatment.

inhibits and/or reverses tumor progression. When we used the progression protocol (Fig. 2A, *b*), gefitinib treatments were started 12 weeks after exposure to BaP and terminated at 20 weeks after BaP. It was continued for a total of 8 weeks and no significant body weight loss was observed at the dose of 200 mg/kg. Gefitinib significantly reduced tumor multiplicity by 59.7% when compared with control group (Fig. 3C). On the total tumor load, the treatment of gefitinib showed even more striking effects. It decreased the tumor load by 81.4% when compared with control group (Fig. 3D). Gross and microscopic features of lung tumors from mice with or without gefitinib treatment are shown in Fig. 2B. All tumors seen in gefitinib-treated group were lung adenomas. Lung adenocarcinomas in control group are composed of cells with varying degrees of differentiation, with most cells appearing relatively undifferentiated relative to lung adenomas in treated mice (Fig. 2B, *b*). There is a complete loss of normal alveolar architecture, and the nuclear cytoplasmic ratio is increased in the carcinomas. Nuclear crowding and cytologic atypia are present, and there is heterogeneity of growth patterns. These data indicate that gefitinib is a potent chemopreventive and chemotherapeutic agent for lung tumorigenesis.

Mutations in Tyrosine Kinase Domain of EGFR and K-ras

Mutations of EGFR have been reported to respond to gefitinib in humans. The main mutations were either in-frame

[3] http://www.fda.gov/cder/foi/label/2005/021399s008lbl.pdf.
[4] http://www.fda.gov/cder/guidance/5541fnl.pdf.

deletions or amino acid substitutions clustered around the ATP-binding pocket of the tyrosine kinase domain focused on exons 18, 19, and 21 (single-nucleotide substitutions in exons 18 and 21 and in-frame deletions in exon 19; refs. 9, 10). In this study, exons 18, 19, 20, and 21 of EGFR from a series of both normal lungs and lung tumors with or without gefitinib treatment were sequenced by PCR direct sequencing. No mutations in these exons were found in DNAs from 5 control tumors and 5 gefitinib-treated lung tumors from A/J mice as well as from 20 adenomas and 5 adenocarcinomas from *p53* transgenic mice. The results were confirmed in both sense and antisense direction analysis. Next, we determined the presence of K-*ras* mutations in lung tumors from mice with and without gefitinib. Mutation analysis of K-*ras* was done on a total of 11 lung tumors from wild-type mice that were treated with BaP and 9 tumors in mice treated with BaP plus gefitinib. The overwhelming majority of the tumors harbored mutations in the 12th codon of K-*ras*, and there was no significant difference in the incidence of mutation between tumors in mice treated with and without gefitinib [8 of 9 (88.9%) versus 10 of 11 (90.9%); Table 1].

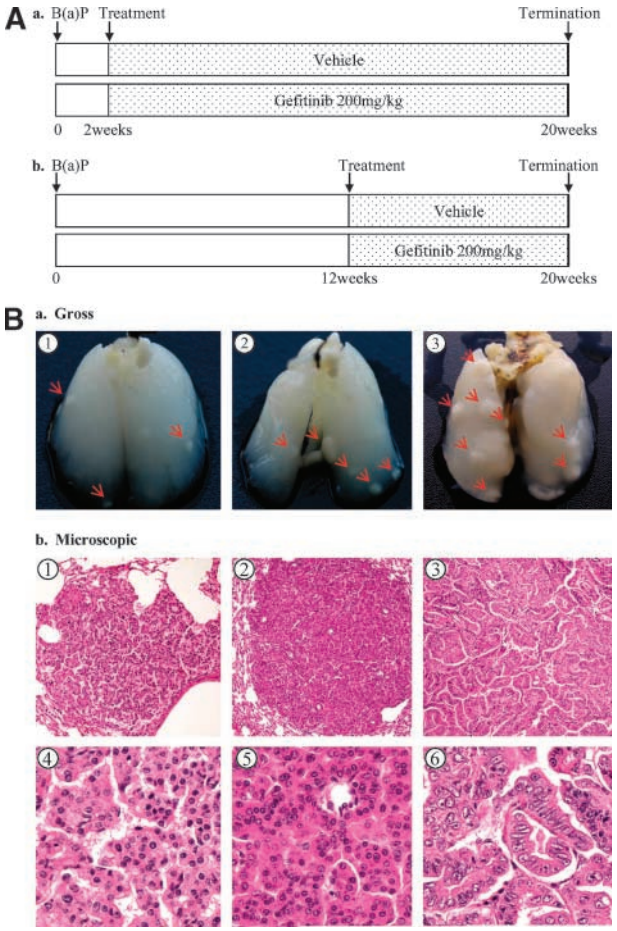

FIGURE 2. Protocol and histopathology. **A.** Protocol for bioassays of gefitinib against BaP-induced lung tumorigenesis. All mice were subjected a single i.p. dose of BaP at 100 mg/kg body weight dissolved in 0.2 mL tricaprylin. **a,** early group: 2 wk after BaP injection, gefitinib treatment group mice [wild-type mice (n = 15) and dominant mutant p53$^{mut/wt}$ mice (n = 15)] were given gefitinib by gavage at the dose of 200 mg/kg body weight in 0.2 mL of 1% Tween 80, five times per week, and continued for 18 wk, whereas control group mice [wild-type mice (n = 12), dominant mutant p53$^{mut/wt}$ mice (n = 13)] were treated with vehicle control. **b,** late group: 12 wk after the BaP injection, gefitinib group mice (n = 25) were given gefitinib by gavage and continued for 8 wk, whereas control group mice (n = 15) were treated with vehicle. All mice were sacrificed at 20 wk after the BaP injection. **B.** Histopathology of pulmonary lesions seen in p53$^{mut/wt}$ mice. **a,** representative lung nodules seen in treated groups (*1*) and in control groups (*2* and *3*). Red arrows, tumors. **b,** light photomicrographs of representative tumors from the treatment group (*1* and *4*) and control groups (*2* and *5* and *3* and *6*) at ×100 and ×400 magnification, respectively.

Expression and Phosphorylation of EGFR

To determine whether protein levels of EGFR are altered between normal lung and BaP-induced lung tumors, samples from each group were subjected to Western blot analysis. EGFR protein expression was not detected in three separate adenocarcinomas (diameter, >3 mm; ref. 15), although EGFR was expressed in two of the three normal lung samples (Fig. 4A). To confirm the result of higher protein level of EGFR in normal tissue than in tumor, we conducted the quantitative real-time PCR analyses for EGFR between normal tissues and BaP-induced lung tumors. The expression of EGFR in normal tissue was 2.64-fold higher than that in BaP-induced lung tumors (Fig. 4B). These results are consistent with the result from the Western blot analysis. We also determined the phosphorylation state of EGFR in the lung tumors and normal lung by Western blot using an antibody specific to phosphorylated Tyr^{1068} of EGFR. Phosphorylation of EGFR in both tissues was not detectable; however, the phosphorylation of an equivalent amount of EGFR was significantly higher in 293T cells (Fig. 4A). This suggests that the phosphorylation levels of EGFR in tumors and normal lung are both very low. Finally, because gefitinib is tyrosine kinase inhibitor and may inhibit other growth factor receptors with tyrosine kinase domain by binding at their ATP site of the tyrosine kinase region, such as vascular endothelial growth factor receptor (VEGFR), fibroblast growth factor receptor (FGFR), platelet-derived growth factor receptor, and insulin-like growth factor receptor (IGFR), the mRNA expression levels of VEGFR, FGFR, platelet-derived growth factor receptor, and IGFR were analyzed using real-time PCR. Similarly, we did not observe increased expression of these growth factor receptors in mouse lung tumors. The mRNA expression in normal lung tissues is 2.83-, 4.00-, 3.72-, and 3.03-fold higher than those in lung tumor tissues in *VEGFR, FGFR, FDGFR*, and *IGFR* target genes, respectively (Fig. 4B).

Oligonucleotide Array Analysis of Lung Tumors and Normal Tissues from Mice Treated with and without Gefitinib

To identify specific genes or pathways that may directly or indirectly contribute to the protective effect of gefitinib on tumorigenesis, three to four independent tumors and normal tissues from gefitinib treatment and control groups were used for this analysis. Oligonucleotide array using Affymetrix GeneChips revealed >3,500 genes that were differentially expressed when comparing control normal lung tissues and control lung tumors (data not shown). Among them, the expression of 208 genes, which were initially underexpressed or

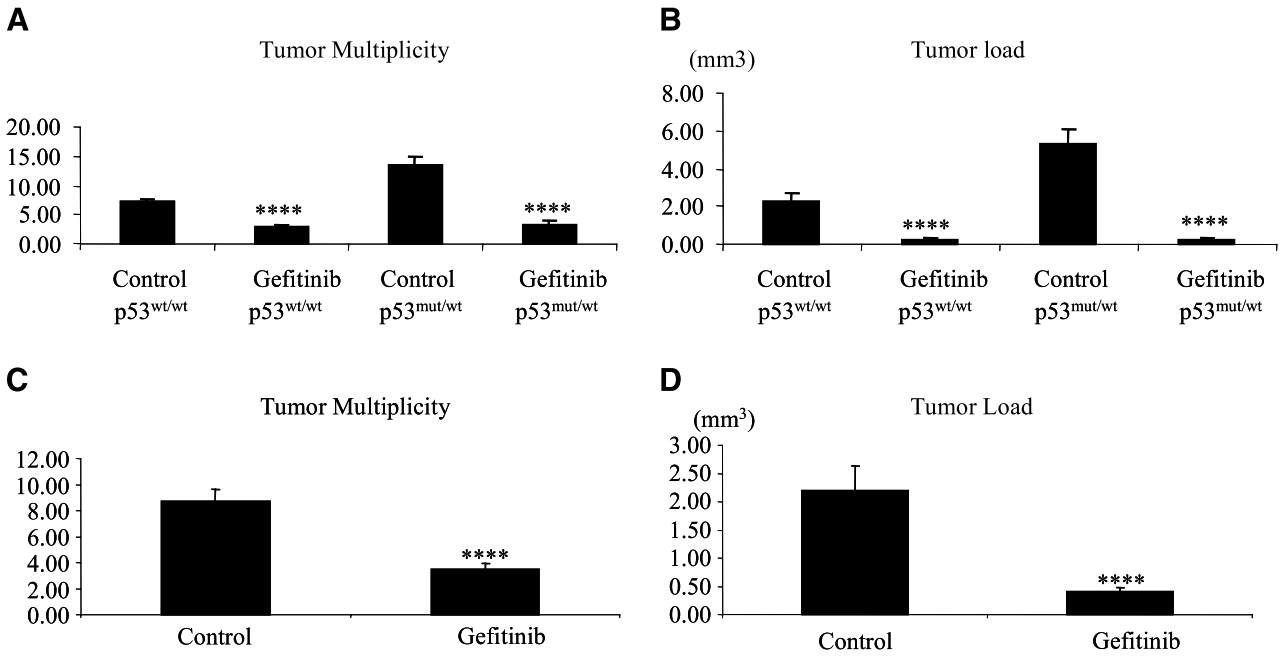

FIGURE 3. Chemopreventive efficacy of gefitinib on BaP-induced lung tumorigenesis in A/J mice. **A** and **B.** Results of tumor multiplicity and tumor load in test early group started 2 wk after BaP injection in wild-type ($p53^{wt/wt}$) and dominant mutant p53 mice ($p53^{mut/wt}$). **C** and **D.** Results in the treatment groups that started 12 wk after BaP injection in A/J mice. **A.** Gefitinib decreased tumor number by 62.5% in wild-type mice [7.27 ± 0.54 (n = 12) versus 2.73 ± 0.46 (n = 15)] and by 74.6% in $p53^{mut/wt}$ mice [13.50 ± 1.25 (n = 13) versus 3.43 ± 0.63 (n = 15)]. **B.** Gefitinib reduced tumor load by 89.3% in wild-type mice [2.24 ± 0.44 mm^3 (n = 12) versus 0.24 ± 0.05 mm^3 (n = 15)] and by 94.9% in $p53^{mut/wt}$ mice [5.31 ± 0.8 mm^3 (n = 13) versus 0.27 ± 0.07 mm^3 (n = 15)]. **C.** Gefitinib reduced tumor number by 59.7% [8.73 ± 0.92 (n = 15) versus 3.52 ± 0.42 (n = 25)] in A/J mice. **D.** Gefitinib reduced tumor load by 81.4% [2.20 ± 0.43 mm^3 (n = 15) versus 0.41 ± 0.07 mm^3 (n = 25)] in A/J mice. Bars, SE. ****, $P < 0.0001$.

overexpressed in control lung tumors, was modulated toward to the normal lung tissue level in gefitinib-treated lung tumors (with the cutoff fold >1.5, $P < 0.05$; Fig. 5A). Among the 208 genes, 71 underexpressed genes were up-regulated and 137 overexpressed genes were down-regulated by gefitinib (Fig. 5A). Genes that were related to tumorigenesis were shown in Table 2. We selected six genes (*Ar, Amid, Rspondin, Fas, G0s2*, and *Csf2rb1*) for confirmation, and all of them were validated by real-time PCR analyses. Expression of *Ar, Amid, Rspondin, Fas*, and *G0s2* was up-regulated toward the control lung normal tissue by gefitinib treatment, whereas expression of *Csf2rb1* was down-regulated to normal tissue (Fig. 5B). GenMAPP search revealed that the levels of expression of several apoptotic genes were increased following gefitinib treatment, which may contribute to the efficacy of gefitinib in this mouse lung model (Fig. 5C). Furthermore, three additional pathways, including cell cycle control, G13 signaling, and transforming growth factor-β signaling, may also be involved in the efficacy of gefitinib against mouse lung tumorigenesis (Supplementary Figs. S1-S3).

We have also compared the gene expression changes in mouse models exposed to gefitinib with those that have been found to predict sensitivity to gefitinib in human NSCLC (16). As shown in Table 3, we found that gefitinib treatment changed the expression levels for 15 of these 131 genes in mice tumors (fold change, >1.5), which correspond to the expression profiles predicting sensitivity to gefitinib in human NSCLC. Among these 15 genes, 8 of them were modulated by gefitinib toward the normal level (fold change, >1.5). These genes may represent common targets of gefitinib in both human and mouse lung tumors.

Table 1. Analysis of K-ras Mutations in Lung Tumors from Mice Treated with Gefitinib or Vehicle

Treatment	Incidence (%)	GGT→TGT	GGT→GTT	GGT→GAT
BaP	10/11 (90.91)	2	6	2
BaP + Gefitinib	8/9 (88.89)	2	2	4

NOTE: There was no significant difference in the incidence of mutation between tumors in mice treated with and without gefitinib.

Discussion

Gefitinib is a small-molecule agent that is recognized as an inhibitor of the tyrosine kinase domain of the EGFR (3, 17, 18). Inhibition of the tyrosine phosphorylation by gefitinib results in decreased activation of various downstream elements (19). Gefitinib and other EGFR inhibitors can induce growth inhibition and growth delay in a wide range of tumor cell lines and human tumor xenografts. In some NSCLC patients, gefitinib can cause remarkably rapid and often profound responses. Small-molecule EGFR inhibitors have been recently approved for clinical use in the treatment of advanced NSCLC as monotherapy following failure of chemotherapy (6). Most of the initial clinical trials with the EGFR inhibitors have used individuals with metastatic disease who have failed standard

therapies (11). Many of those clinical trials have shown limited efficacy as monotherapies (11). However, a more limited number of studies in earlier stages of cancer have shown more striking efficacy, implying that this class of compounds might be more useful in earlier clinical stages or in prevention (11). Interestingly, in advanced lung cancer, the efficacy of the EGFR inhibitors was most effective against tumors with an activating mutations in the tyrosine kinase domain of the EGFR (9, 10). However, some lung tumors without EGFR mutations and other cancers without EGFR mutations have proven sensitive to the EGFR inhibitors as well (11).

In view of the potential interest in the use of EGFR inhibitors in early-stage lung cancer and potentially in a prevention setting, we undertook the studies presented. We conducted a bioassay of gefitinib on BaP-induced lung tumorigenesis in A/J mice that mimic histopathology and stages of tumor progression with human lung adenocarcinomas (13, 14). Gefitinib was well tolerated throughout the duration of the experiment (Fig. 1). We used two different prevention protocols to examine the chemopreventive efficacy. The first protocol entailed treatment with gefitinib beginning 2 weeks after BaP for 18 weeks. In wild-type or $p53^{mut/wt}$ mice, this resulted in profound decreases in tumor multiplicity (62% and 75%; Fig. 3A) and even more striking decreases in tumor volume (89 and 94%; Fig. 3B). Our second protocol done only in wild-type mice resulted in significantly decreased tumor multiplicity and volume (59.7% and 81.4%, respectively; Fig. 3C and D) despite the fact that treatment was started 12 weeks after the carcinogenic initiation with BaP. At 12 weeks after the BaP injection, multiple preinvasive lesions have developed in lung tissues. Based on our prior experience, lung adenomas tend to have tumors <1 mm in diameter, whereas lung adenocarcinomas will tend to have tumors >3 mm (15). In view of the striking decrease in average size of the tumors in the gefitinib group, this implies a striking change in the incidence of adenocarcinomas. These results have two important findings. Gefitinib was highly effective in lesions with or without a *p53* mutation when given early. More importantly, late administration in wild-type mice was similarly effective as early treatment, implying that most of the effect occurs later during the progression stage, which is important because this is the most likely treatment protocol clinically. These results show that gefitinib can strongly inhibit and potentially reverse the process of lung tumorigenesis.

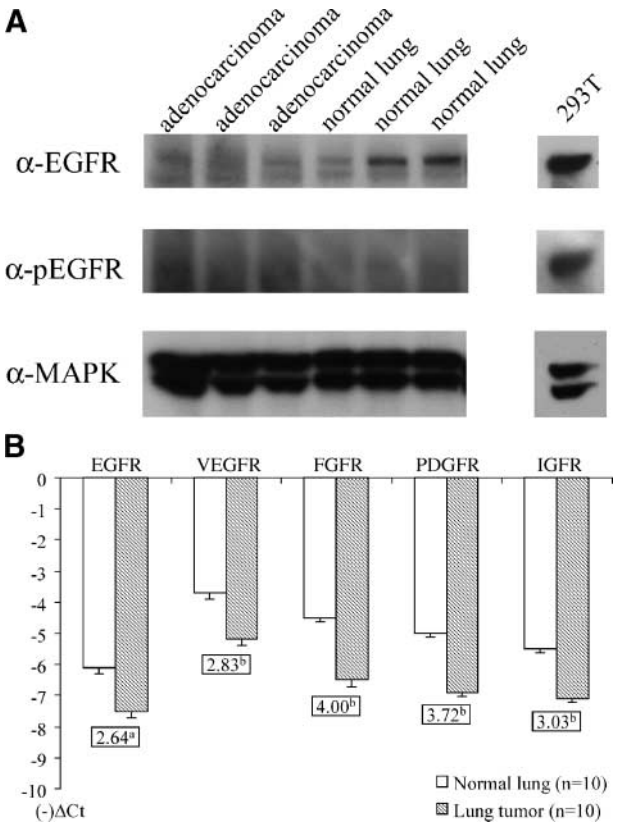

FIGURE 4. EGFR and other growth factor receptors in mouse lung tumors. **A.** Protein level and phosphorylation status of EGFR in normal tissue and BaP-induced lung adenocarcinomas by Western blot analysis. The diameters of tumors were >3 mm. α-MAPK was used as internal control. **B.** Results of relative gene expression of growth factor receptors by real-time PCR. Columns, mean $-\Delta C$t values (threshold cycle of GAPDH minus threshold cycle for target gene); bars, SE. There were 10 samples in each group for normal lung and lung tumor. Numbers in boxes, fold changes. The mRNA expression in normal lung tissues is 2.64-, 2.83-, 4.00-, 3.72-, and 3.03-fold higher than those in lung tumor tissues in *EGFR, VEGFR, FGFR, platelet-derived growth factor receptor* (*PDGFR*), and *IGFR* target genes, respectively. a, $P < 0.001$; b, $P < 0.00001$.

Activating mutations of EGFR tyrosine kinase domain have been reported to dramatically increase the response to gefitinib treatment in human lung cancer patients, although a significant number of tumors without such mutations were responsive as well (9, 10). The main mutations were either in-frame deletions or amino acid substitutions clustered around the ATP-binding pocket of the tyrosine kinase domain focused on exons 18, 19, and 21 (single-nucleotide substitutions in exons 18 and 21 and in-frame deletions in exon 19). Based on our prior experience, lung adenomas tend to have tumors <1 mm in diameter, whereas lung adenocarcinomas will most likely consists of tumors >3 mm (15). Accordingly, we sequenced the same regions flanking exons of 18, 19, 20, and 21 from 5 control normal lungs, 5 gefitinib-treated normal lungs, 5 control tumors, 5 treated tumors, 5 large BaP-induced tumors (>3 mm in diameter), and 20 small BaP-induced tumors (<1 mm in diameter). In both sense and antisense sequence analysis, we could not find mutations with these samples in exons 18, 19, 20, and 21. Gefitinib had activities in several cancer types, including recurrent glioblastoma, where there are no mutations in the EGFR tyrosine kinase region (20). There were no detectable levels of phosphorylated EGFR in mouse lung tumors examined, which is the primary postulated target of these EGFR inhibitors (Fig. 4A). To determine whether protein levels of EGFR differed between normal lung and BaP-induced lung tumors, we did Western blot analysis. We found that the expression levels in normal tissue were much higher than that in adenocarcinomas (Fig. 4A). The relative mRNA expression analysis of EGFR by real-time PCR also indicated that high expression of EGFR is probably not needed for the efficacy. The results were consistent with the finding that the efficacy of gefitinib in tumorigenesis was not dependent on the expression level or phosphorylation status of EGFR (4, 21). EGFR belongs

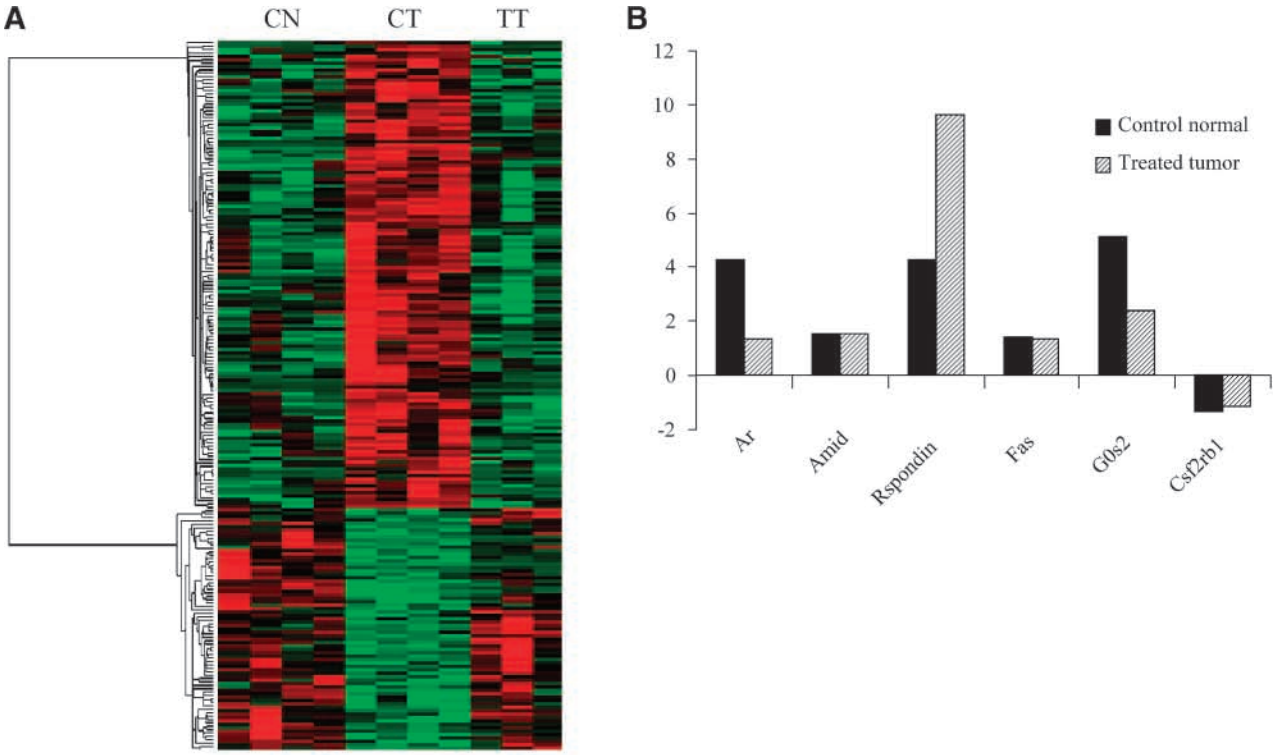

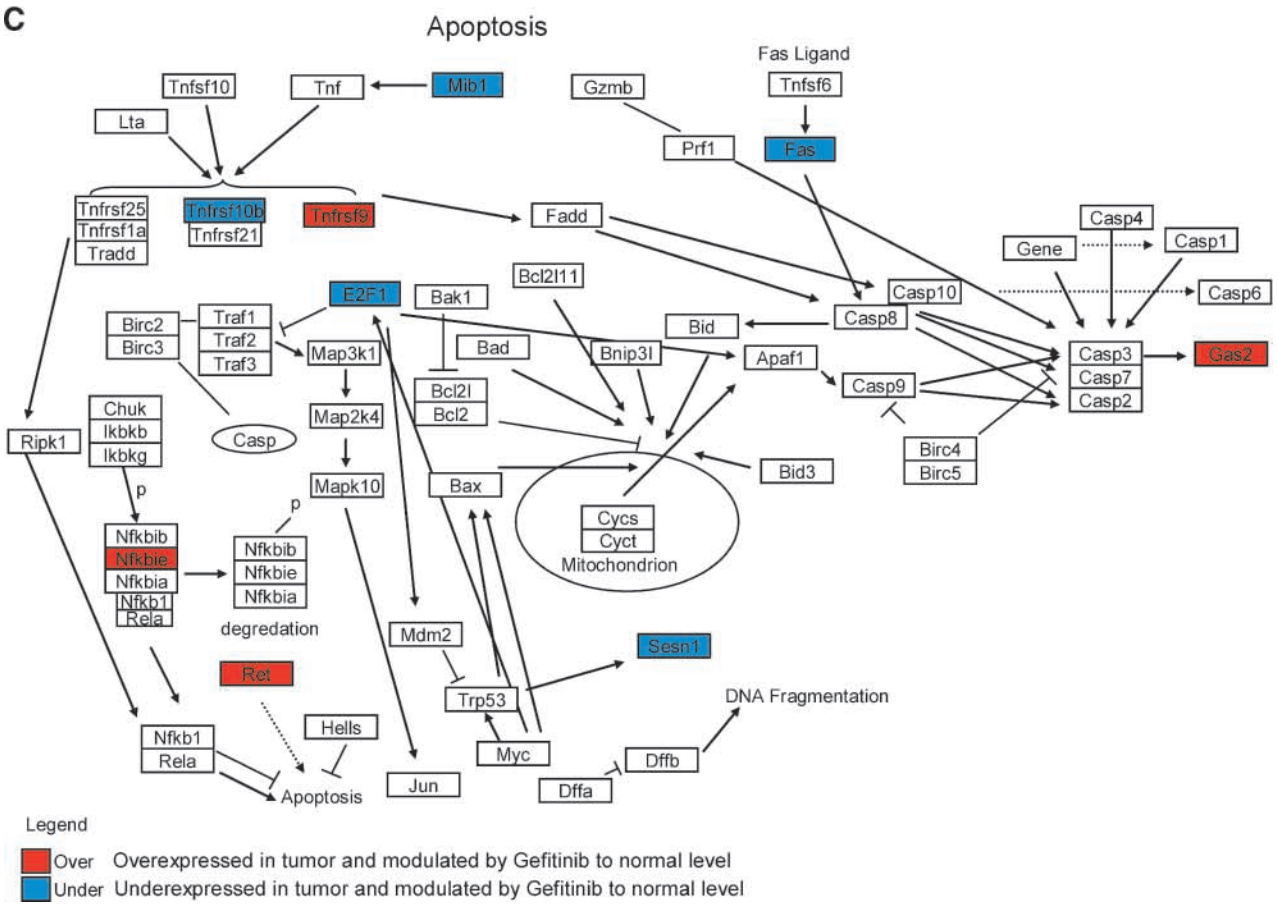

Table 2. Selected Genes with Significant Down-Regulated or Up-Regulated Expression Levels in Lung Tumorigenesis by Gefitinib Treatment toward the Expression Levels of the Normal Tissues

Probe set	Accession no.	Unigene gene name	Symbol	Expression levels			Fold	
				CN	CT	TT	CT/CN	TT/CT
				Up	Down	Up		
1435486_at	BQ175796	P21 (CDKN1A)-activated kinase 3	*Pak3*	225	29	129	−7.8	4.5
1442159_at	C77557	E2F transcription factor 1	*E2f1*	227	44	298	−5.2	6.8
1437064_at	AV232123	Androgen receptor	*Ar*	871	173	409	−5.0	2.4
1444008_at	BB396393	Apoptosis-inducing factor–like mitochondrion-associated inducer of death	*Amid*	346	93	317	−3.7	3.4
1422344_s_at	NM_020294	Tumor necrosis factor receptor superfamily, member 10b	*Tnfrsf10b*	189	62	272	−3.1	4.4
1432957_at	AK017518	Cdc42 guanine nucleotide exchange factor 9	*Arhgef9*	97	33	208	−3.0	6.3
1449129_a_at	AF300870	Calsenilin, presenilin binding protein, EF hand transcription factor	*Csen*	155	55	213	−2.8	3.9
1449319_at	NM_138683	Thrombospondin type 1 domain containing gene	*Rspondin*	1,245	476	773	−2.6	1.6
1456676_a_at	AV282911	6-Phosphofructo-2-kinase/fructose-2,6-biphosphatase 3	*Pfkfb3*	529	218	329	−2.4	1.5
1460251_at	NM_007987	Fas (tumor necrosis factor receptor superfamily member)	*Fas*	3,541	1,465	2,899	−2.4	2.0
1444376_at	BM237933	Sestrin 1	*Sesn1*	329	149	254	−2.2	1.7
1424523_at	BC024727	Engulfment and cell motility 1, ced-12 homologue (*Caenorhabditis elegans*)	*Elmo1*	2,153	1,026	1,642	−2.1	1.6
1434957_at	AW557006	Cell adhesion molecule-related/down-regulated by oncogenes	*Cdon*	1,036	566	913	−1.8	1.6
1417938_at	BC003738	RAD51 associated protein 1	*Rad51ap1*	1,220	766	1,198	−1.6	1.6
1451818_at	BC011287	Mindbomb homologue 1 (*Drosophila*)	*Mib1*	525	339	668	−1.5	2.0
1448700_at	NM_008059	G_0-G_1 switch gene 2	*G0s2*	5,717	3,727	5,691	−1.5	1.5
				Down	Up	Down		
1422301_at	NM_008049	Ferritin light chain 2	*Ftl2*	2,403	3,838	2,292	1.6	−1.7
1450200_s_at	NM_007780	Colony stimulating factor 2 receptor, β1, low affinity (granulocyte-macrophage)	*Csf2rb1*	598	1,014	570	1.7	−1.8
1431843_a_at	AK011965	Nuclear factor of κ light polypeptide gene enhancer in B-cell inhibitor, ϵ	*Nfkbie*	611	1,106	665	1.8	−1.7
1450014_at	NM_016674	Claudin 1	*Cldn1*	338	619	339	1.8	−1.8
1421359_at	NM_009050	Ret proto-oncogene	*Ret*	251	462	242	1.8	−1.9
1438767_at	BB237825	Oncostatin M	*Osm*	357	671	273	1.9	−2.5
1434812_s_at	BB752451	Oncoprotein-induced transcript 5	*Oit5*	390	736	398	1.9	−1.8
1442225_at	BE952870	Cell division cycle 2-like 6 (CDK8-like)	*Cdc216*	114	223	41	1.9	−5.4
1439383_x_at	BB558642	Protein phosphatase 2A, regulatory subunit B (PR 53)	*Ppp2r4*	303	599	247	2.0	−2.4
1418237_s_at	NM_009929	Procollagen, type XVIII, α1	*Col18a1*	1,485	2,965	1,925	2.0	−1.5
1422462_at	NM_026024	Ubiquitin-conjugating enzyme E2T (putative)	*UBE2T*	221	462	293	2.1	−1.6
1439602_at	BB344218	Fidgetin	*Fign*	140	294	99	2.1	−3.0
1459761_x_at	BB342841	Immunoglobulin superfamily, member 4d	*Igsf4d*	210	463	302	2.2	−1.5
1421623_at	NM_008354	Interleukin 12 receptor, β 2	*Il12rb2*	111	249	94	2.2	−2.6
1416916_at	NM_007921	E74-like factor 3	*Elf3*	1,365	3,148	1,991	2.3	−1.6
1432429_at	AK018473	Dachshund 1 (*Drosophila*)	*Dach1*	99	242	71	2.4	−3.4
1422285_at	NM_011021	Orthopedia homologue (*Drosophila*)	*Otp*	82	212	85	2.6	−2.5
1438564_at	BM507943	Growth arrest specific 2	*Gas2*	96	264	65	2.7	−4.0
1420576_at	NM_020028	Endothelial differentiation, lysophosphatidic acid G protein–coupled receptor 4	*Edg4*	119	438	175	3.7	−2.5
1460469_at	BM250782	Tumor necrosis factor receptor superfamily, member 9	*Tnfrsf*	283	1,177	382	4.2	−3.1

NOTE: The genes located at the upper panel have a decreased expression patterns during tumorigenesis, and gefitinib treatment up-regulated the gene expression toward normal levels. The genes located at the lower part have an increased expression patterns during tumorigenesis, and the gefitinib treatment down-regulated the gene expression toward to normal expression levels.
Abbreviations: CN, control normal tissue; CT, control tumor; TT, gefitinib-treated tumor.

to the ErbB family of tyrosine kinase protein. This family includes four members: EGFR, ErbB-2/Neu/HER2, ErbB-3/HER3, and ErbB-4/HER4. The members of the ErbB family have a similar structure with high degree of homology in the tyrosine kinase domain (18). Their homodimeric and heterodimeric dimerization is followed by activation of intrinsic protein tyrosine kinase activity, tyrosine phosphorylation, and activation of intracellular signal transduction pathway, such as phosphatidylinositol 3-kinase/AKT and ras/raf/MAPK/extracellular signal-regulated kinase kinase/MAPK pathway (22). It is possible that despite the absence of EGFR mutations in kinase domain and no detectable expression in tumors, gefitinib treatment dramatically reduced both the number and size of tumor nodules following exposure to a known carcinogen

FIGURE 5. Microarray analyses of tissues treated with gefitinib. **A.** Hierarchical clustering of 208 genes and expressed sequence tags that were modulated by gefitinib toward the normal level. CN, control normal tissue; CT, control tumor; TT, treated tumor. Among the 208 genes, 137 genes show the down-up-down and 71 genes show the up-down-up patterns for the normal tissue-control tumor-gefitinib-treated tumor. **B.** Results of confirmation of Affymetrix GeneChip probe array by real-time PCR. The results show the fold changes compared with control tumor. Genes of *Ar, Amid, Rspondin, Fas, G0s2*, and *Csf2rb1* showed reduced expression level in control tumor tissues and were modulated by gefitinib treatment toward levels in control normal tissues. The expression of *Csf2rb1* was increased in control tumor compared with control normal and reversed by the treatment to normal level. There were five samples in each group for control lung, control tumor, and gefitinib-treated lung tumor. **C.** GenMAPP apoptosis pathways integrating our expression data (cutoff: fold change, >1.5). Red, overexpressed genes in BaP-induced tumors were modulated to normal levels after gefitinib treatment; blue, underexpressed genes in BaP-induced tumors were modulated to normal levels after gefitinib treatment.

Table 3. Corresponding Genes Sensitive to Gefitinib in Both Mouse and Human Tumors

Mouse model						Human NSCLC		
Symbol	Probe set	Expression levels			Fold change (TT/CT)	Symbol	Genbank ID	Expressed class
		CN	CT	TT				
Areg	1421134_at	468	2,412	1,439	−1.68	AREG	BC009799	PD
Dusp3	1425608_at	1,432	1,444	951	−1.52	DUSP3	NM_004090	PD
Nasp	1440328_at	155	131	314	2.40	NASP	AF113699	PR
Smad3	1450471_at	161	263	45	−5.84	SMAD3	NM_005902	PD
Fmn1	1427671_a_at	12	21	149	7.09	FMN1	AA059467	PR
Tbc1d16	1442149_at	247	425	71	−5.98	TBC1D16	AA531128	PD
Ap1g1	1460658_at	27	89	8	−11.13	AP1G1	Y12226	PD
Gpt2	1438385_s_at	621	1,461	896	−1.63	GPT2	AI356291	PD
Cdkn2c	1439164_at	11	17	29	1.71	CDKN2C	AI357641	PR
Pten	1441593_at	124	195	28	−6.96	PTEN	BC005821	PD
Baiap2	1435128_at	294	274	156	−1.76	BAIAP2	AI339146	PD
Foxm1	1448833_at	707	786	53	−14.83	FOXM1	BC006192	PD
Tgfa	1421942_s_at	67	205	39	−5.26	TGFA	NM_003236	PD
St13	1442775_at	429	302	168	−1.80	ST13	NM_003932	PD
Eif4g2	1458431_at	479	728	484	−1.50	EIF4G2	X89713	PD

NOTE: By using a genome-wide cDNA microarray to analyze 33 biopsy samples of advanced NSCLC from patients who had been treated with gefitinib, Kakiuchi et al. (16) identified 131 genes whose expression differed significantly between 7 responders and 10 nonresponders to the drug. We found that gefitinib treatment changed the expression levels for 15 of these 131 genes in mice tumors (fold change, >1.5), which correspond to the expression profiles predicting sensitivity to gefitinib in human NSCLC. Among these 15 genes, 8 of them were modulated by gefitinib toward to the normal level (fold change, >1.5). Symbol in bold font: genes modulated by gefitinib toward the normal level.

would suggest that in fact the mechanism of the chemoprevention of gefitinib may be related to other ErbB family members, such as ErbB-2, ErbB-3, and ErbB-4. It has been proved that gefitinib is able to affect signal transduction through different ErbB receptors (18).

To identify specific genes or pathways that may directly or indirectly contribute to the protective effect of gefitinib on gene expression in lung tumors from control and gefitinib-treated mice was investigated. Oligonucleotide array together with GenMAPP analysis revealed that gefitinib affects several cellular processes involved in the tumorigenesis, including apoptosis, cell cycle, cell proliferation, cell transformation, angiogenesis, DNA synthesis, cell migration, immune responses, etc. (Table 2). They are involved in the E2F pathway, tumor necrosis factor pathway, Fas pathway, nuclear factor-κB (NF-κB) pathway, caspase pathway, etc. Many of them are related to the process of apoptosis (Fig. 5C). Specifically, *E2F1, Tnfrsf10b, Fas, Sesn1, Mib1, Nfkbi2, Ret*, and *Tnfrsf9* are found to be modulated toward levels observed in control normal lung. For example, *E2F1* can induce apoptosis by a death receptor–dependent mechanism and by down-regulating *Traf2* protein levels and inhibiting activation of antiapoptotic signals, such as *NF-κB* (23). *E2F1* also can induce p53-dependent apoptosis by inducing *ARF* (CDKN2A), which neutralizes *Mdm2* and stabilizes *p53* that similarly may induce apoptosis (24). *E2F1* can bind with the promoter region of human *Apaf1* and induce apoptosis accompanied by *casp9* (25). In this study, *E2F1* was expressed at very low level in control tumors, whereas the gefitinib treatment up-regulated the expression by ~7-fold (Table 2). Similarly, *Fas* belongs to tumor necrosis factor receptor superfamily. It activates *caspase-3* (26) and *caspase-8* for the cascade of caspases to lead to apoptosis (27). In the BaP-induced lung tumor, the expression level was 2.4-fold lower than normal tissue. The treatment with gefitinib reversed the expression toward to the normal level (Table 2). *NF-κB* transcription factor has been detected in numerous cell types that express cytokines, chemokines, growth factors, cell adhesion molecules, and some acute phase proteins in health and in various disease states. It can protect from or contribute to apoptosis. It was reported that complete and persistent inhibition of *NF-κB* has been linked directly to apoptosis (28). In contrast, in cells without *NF-κB* activity, p53-induced apoptosis was abrogated (29). IκB proteins (*Nfkbia, Nfkbib*, and *Nfkbie*) inactivate *NF-κB* by trapping it in the cytoplasm. They are necessary to generate the characteristic *NF-κB* activation profile (30). In this study, the expression level of *Nfkbie* was down-regulated by gefitinib to normal level (Table 2). Interestingly, gefitinib treatment changed the expression levels for 15 of those 131 genes (16) in mice tumors (fold change, >1.5; Table 3), which

Table 4. Oligonucleotide Primers Used in the PCR Direct Sequencing for EGFR in Exons 18, 19, 20, and 21

	Forward primer	Reverse primer	Product size (bp)
Exon 18	CTCTGGCTCAGAATGAATCTAC	GAAGCCTAGTGCGGACCTGTC	268
Exon 19	CCAGCTCACAAGGCAACATG	CTAAGGAAGCAAGATTGACC	229
Exon 20	GATTCATCTATTGTCCTTACC	TGGGTACTTCAGTGGACAGAC	234
Exon 21	CATGACACTGAGGATGCCCAGA	CAAATGCTGCCCACAGCTGAC	298

NOTE: The sequences were based on the data in the Web site (http://www.ensembl.org/Mus_musculus/index.html) with transcript ID ENSMUST00000020329.

Table 5. Oligonucleotide Primers for Real-time PCR

	Forward primer	Reverse primer	Accession no.
GAPDH	GGGTGTGAACCACGAGAAAT	GTCATGAGCCCTTCCACAAT	NM_008084
EGFR	TTGGCCTATTCATGCGAAGAC	GAGGTTCCACGAGCTCTCTCTCT	NM_207655
VEGFR	TCGGCTGTCCATGAAAGTGA	TTGCAGGCGAGCCATCTT	NM_008029
FGFR	TGGCCAATGTTTCTGAACTTGA	GCCGGGTCCTGGATAGCT	NM_008010
PDGFR	GATGATCTGCAAGCATATTAAGAAATGTA	GGCGAGGGAGCTCTGTGATA	NM_011058
IGFR	CAGCACCCAGAGCATGTACTGTA	TCATCGCCGCAGACTTTG	NM_010513

NOTE: All the sequences were based on the published data on National Center for Biotechnology Information followed by the accession number. GAPDH was used as an internal control.
Abbreviation: PDGFR, platelet-derived growth factor receptor.

correspond to the expression profiles predicting sensitivity to gefitinib in human NSCLCs (16). Among them, eight were modulated by gefitinib toward to the normal level (fold change, >1.5). These genes may represent the common targets of gefitinib in both human and mouse lung tumors.

In summary, this study examined the effect of gefitinib on inhibiting pulmonary carcinogenesis in the A/J strain of mice, which is susceptible to lung tumor induction by chemical carcinogens, and in a *p53*-mutant strain of mouse. Gefitinib was able to inhibit tumor multiplicity and tumor size to a high extent whether given beginning 2 weeks or beginning 12 weeks after carcinogen treatment. Consistent mutation in K-*ras* was found in tumors that arose in both the placebo-treated and gefitinib-treated lungs. Gefitinib altered gene expression in a reproducible way for genes involved in cell growth and cell death. In many of the human studies in metastatic NSCLC, mutations in K-*ras* seemed to predict a lack of response to gefitinib (31). Thus, concurrent EGFR mutations and K-*ras* mutations were virtually never observed (31). However, the A/J lung tumor model has K-*ras* mutations in virtually 100% of the tumors examined either in wild-type or $p53^{mut/wt}$ animals. Despite this lack of EGFR mutations and presence of K-*ras* mutations, we observed striking efficacy in both wild-type and *p53*-mutant animals even when gefitinib was used late during tumor progression. This is the first report of a chemopreventive effect of an EGFR inhibitor in mouse models of lung cancer. The results suggest that inhibiting EGFR may have potential as a chemopreventive approach.

Materials and Methods

Reagents and Animals

BaP (99% pure) and tricaprylin were purchased from Sigma Chemical Co. (St. Louis, MO). Gefitinib was obtained from Chemoprevention Branch, National Cancer Institute (Bethesda, MD). A/J female mice at 6 weeks of age were obtained from The Jackson Laboratory (Bar Harbor, ME). The use of animals was approved by the Institutional Animal Care and Use Committee of the Washington University (St. Louis, MO).

Preliminary Toxicology of Gefitinib in A/J Mice

A preliminary toxicity study was conducted with gefitinib (Fig. 1A), and a dose of 200 mg/kg body weight did not cause mortality or significantly affect body weight. Briefly, A/J female mice were divided into five dose groups: control, 100 mg/kg (32), 200 mg/kg, 300 mg/kg, and 400 mg/kg for gefitinib treatment by gavage, five times per week, in 0.2 mL of 1% Tween 80 solution. Five animals were used in each testing group. Animals were housed in plastic cages with hardwood bedding and dust covers in a high-efficiency particulate air–filtered, environmentally controlled room ($24 \pm 1^{\circ}C$, 12-h light/12-h dark cycle). Body weight was monitored weekly for the duration of the studies. All food and water were available *ad libitum*.

Chemoprevention Studies

The A/J female mice were obtained from The Jackson Laboratory. A total of 95 mice was used in this study with 12 to 25 mice per group. Mice were given a single i.p. dose of BaP (100 mg/kg body weight, prepared just before injection) in 0.2 mL tricaprylin. Two or 12 weeks following the BaP injection, mice were randomized into vehicle control group and gefitinib treatment group. Treatments were initiated and continued for 18 or 8 weeks (Fig. 2A). In testing group, mice were given gefitinib at the dose of 200 mg/kg in 0.2 mL of 1% Tween 80 by gavage based on our preliminary toxicology results five times per week. The justification for the use of a 200 mg/kg dose of gefitinib five times per week is because it is the maximum tolerated dose that did not significantly affect body weight over an 8-week period. If this dosage is highly effective, future experiments will use the 200 mg/kg as a control to determine the effect of lowering doses to 100 or 50 mg/kg. In the control group, mice were give vehicle of 1% Tween 80 only. The body weight was measured every 2 weeks for the duration of the treatment. Mice were killed 20 weeks after exposure to carcinogen of BaP by CO_2 asphyxiation. Portions of tumor and normal tissue were frozen in liquid nitrogen and then transferred to $-80^{\circ}C$ until use. The remaining lung was fixed in Tellyesniczky's solution (15) overnight followed by 70% ethanol. The fixed lungs were evaluated by at least two investigators under a dissecting microscope to obtain the fixed surface tumor count, and individual tumor load was measured for volume calculation based on the following formula: $mm^3 = V = 4 / 3\pi r^3$. The total tumor load was obtained by adding the individual tumor load per lung, and the total tumor count was obtained by adding the individual tumor count per lung.

Analysis of Mutations in the 18, 19, 20, and 21 Exons of EGFR by PCR Direct Sequencing

DNA was isolated from five samples in each of control normal tissue, control tumor, gefitinib-treated lung tissue, and

treated tumor from the postinitiation protocol using the Trizol (Invitrogen, Carlsbad, CA). We also used DNA samples from BaP-induced lung tumors in p53 transgenic mice, including 20 adenomas (diameter, <1 mm) and 5 adenocarcinoma (diameter, >3 mm) from another bioassay (15). Sequences of PCR primers for EGFR were based on the data on the Web site[5] with transcript ID ENSMUST00000020329 (Table 4). PCR mixtures with DNA template were subjected to 35 cycles of PCR amplification. Each cycle consisted of 1 min each at 95°C, 51°C, and 72°C. PCR products were resolved on 1.5% ethidium bromide–stained agarose gels and purified using QIAquick gel extraction kits (Qiagen Sciences, Germantown, MD). All the PCR fragments were automatically sequenced in both sense and antisense directions in the Protein and Nucleic Acid Chemistry Laboratories of Washington University by using Applied Biosystems Models 3100 and 3730 DNA sequencers (Perkin-Elmer, Foster City, CA). The mutations of 18, 19, 20, and 21 exons in EGFR were analyzed with the Sequencher software version 4.0.5 (Gene Codes Corp., Ann Arbor, MI).

Protein Levels of EGFR in Normal Lung Tissue and BaP-Induced Tumor

Samples of extracted normal lung and lung tumors were Dounce homogenized in PBS in the presence of 1 mmol/L DTT, Complete protease inhibitor cocktail (Roche, Indianapolis, IN), and phosphatase inhibitor cocktail I and II (Sigma). Triton X-100 was added to a final concentration of 1%, and lysates remained on ice for 10 min. Lysates were centrifuged at 13,000 × *g* at 4°C. The supernatants were collected and added to lithium dodecyl sulfate sample buffer (Invitrogen) and 50 mmol/L DTT. Samples were electrophoresed on a 4% to 12% NuPAGE (Invitrogen) gel, transferred to polyvinylidene difluoride, and blotted with the indicated antibodies (EGFR, phosphorylated EGFR, and MAPK; Cell Signaling Technology, Danvers, MA). MAPK was used for internal control.

Quantitative Real-time PCR Analysis

Relative gene expressions of EGFR (NM_207655), VEGFR (NM_008029), FGFR (NM_008010), platelet-derived growth factor receptor (NM_011058), and IGFR (NM_010513) were determined by quantitative real-time PCR analysis (33). The primers shown on Table 5 were designed using PrimerExpress version 2.0 (Applied Biosystems, Foster City, CA). Amplification of each target cDNA was done with SYBR Green Master Mix in Bio-Rad (Hercules, CA) Single-Color Real-time PCR Detection System according to the protocols provided. The control gene *glyceraldehyde-3-phosphate dehydrogenase* (*GAPDH*) and target genes were amplified with equal efficiencies, and the $-\Delta Ct$ ($-\Delta Ct = Ct$ GAPDH gene $- Ct$ target gene) values were used to quantitate the logarithmic transformation of the mRNA level of the target gene relative to that of GAPDH (33).

Affymetrix GeneChip Probe Array

Total RNA from each sample was isolated by Trizol according to the manufacturer's protocols. Then, the samples of RNA were treated at GeneChip Core Facility in Washington University. Labeled cRNA was applied to the Affymetrix MOE430+2 GeneChips (Affymetrix), which contain 45,101 genes and expressed sequence tags on one array. Four samples in control normal lung and control tumor groups and three samples in gefitinib-treated tumor group were used for this array analysis. For each sample in control tumor and treated tumor, one to four tumors were combined (pooled) based on their size.

Cluster and GenMAPP

Four or three independent tumor samples were collected for each group. Array normalization and gene expression estimates were obtained using Affymetrix Microarray Suite 5.0 software. Differential expression was determined on the combined basis of statistical testing using *t* test and based on ratio with a cutoff of $P < 0.05$ and fold >1.5 being called positive for differential expression. For the selected genes, expression indexes were transformed across samples to an $N(0, 1)$ distribution using a standard statistical *Z*-transform. These values were input to the GeneCluster program as reported (15), and genes were clustered using average linkage and correlation dissimilarity. Signal transduction pathways and other functional groupings of genes were evaluated for differential regulation using the visualization tool GenMAPP (University of California at San Francisco).[6] It is a recently reported tool for visualizing expression data in the context of biological pathways (34). We imported the statistical results of our data set into the program and used GenMAPP to illustrate pathways containing differentially expressed genes (15). Differential gene expression was based on gefitinib treatment versus nontreatment expression change (fold change, >1.5).

Statistical Analysis

Tumor multiplicity and tumor load were analyzed by two-sided Student's *t* test using Microsoft Excel 2002 Service Pack 3 to determine the differences in the number and size of lung tumors per mouse between each group. In all *t* tests, the level of statistical significance was set at $P < 0.05$.

[5] http://www.ensembl.org/Mus_musculus/index.html.

[6] http://www.genmapp.org.

References

1. Jemal A, Tiwari RC, Murray T, et al. Cancer statistics, 2004. CA Cancer J Clin 2004;54:8–29.

2. American Cancer Society Surveillance Research. Cancer facts and figures 2004. Atlanta (GA): American Cancer Society; 2004. p. 1–60.

3. Barker AJ, Gibson KH, Grundy W, et al. Studies leading to the identification of ZD1839 (IRESSA): an orally active, selective epidermal growth factor receptor tyrosine kinase inhibitor targeted to the treatment of cancer. Bioorg Med Chem Lett 2001;11:1911–4.

4. Wakeling AE, Guy SP, Woodburn JR, et al. ZD1839 (Iressa): an orally active inhibitor of epidermal growth factor signaling with potential for cancer therapy. Cancer Res 2002;62:5749–54.

5. Moulder SL, Yakes FM, Muthuswamy SK, Bianco R, Simpson JF, Arteaga CL. Epidermal growth factor receptor (HER1) tyrosine kinase inhibitor ZD1839 (Iressa) inhibits HER2/neu (erbB2)-overexpressing breast cancer cells *in vitro* and *in vivo*. Cancer Res 2001;61:8887–95.

6. Cohen MH, Williams GA, Sridhara R, et al. United States Food and Drug Administration Drug Approval summary: gefitinib (ZD1839; Iressa) tablets. Clin Cancer Res 2004;10:1212–8.

7. Kris MG, Natale RB, Herbst RS, et al. Efficacy of gefitinib, an inhibitor of the epidermal growth factor receptor tyrosine kinase, in symptomatic patients with non-small cell lung cancer: a randomized trial. JAMA 2003; 290:2149–58.

8. Fukuoka M, Yano S, Giaccone G, et al. Multi-institutional randomized phase II trial of gefitinib for previously treated patients with advanced non-small-cell lung cancer (The IDEAL 1 Trial) [corrected]. J Clin Oncol 2003; 21:2237–46.

9. Lynch TJ, Bell DW, Sordella R, et al. Activating mutations in the epidermal growth factor receptor underlying responsiveness of non-small-cell lung cancer to gefitinib. N Engl J Med 2004;350:2129–39.

10. Paez JG, Janne PA, Lee JC, et al. EGFR mutations in lung cancer: correlation with clinical response to gefitinib therapy. Science 2004;304:1497–500.

11. Ganti AK, Potti A. Epidermal growth factor inhibition in solid tumours. Expert Opin Biol Ther 2005;5:1165–74.

12. You M, Bergman G. Preclinical and clinical models of lung cancer chemoprevention. Hematol Oncol Clin North Am 1998;12:1037–53.

13. Herzog CR, Lubet RA, You M. Genetic alterations in mouse lung tumors: implications for cancer chemoprevention. J Cell Biochem Suppl 1997;29:49–63.

14. Malkinson AM. Primary lung tumors in mice: an experimentally manipulable model of human adenocarcinoma. Cancer Res 1992;52:2670–6s.

15. Zhang Z, Wang Y, Yao R, et al. Cancer chemopreventive activity of a mixture of Chinese herbs (antitumor B) in mouse lung tumor models. Oncogene 2004;23: 3841–50.

16. Kakiuchi S, Daigo Y, Ishikawa N, et al. Prediction of sensitivity of advanced non-small cell lung cancers to gefitinib (Iressa, ZD1839). Hum Mol Genet 2004; 13:3029–43.

17. Ranson M. ZD1839 (Iressa): for more than just non-small cell lung cancer. Oncologist 2002;4:16–24.

18. Normanno N, Maiello MR, De Luca A. Epidermal growth factor receptor tyrosine kinase inhibitors (EGFR-TKIs): simple drugs with a complex mechanism of action? J Cell Physiol 2003;194:13–9.

19. Ranson M, Mansoor W, Jayson G. ZD1839 (IRESSA): a selective EGFR-TK inhibitor. Expert Rev Anticancer Ther 2002;2:161–8.

20. Rich JN, Reardon DA, Peery T, et al. Phase II trial of gefitinib in recurrent glioblastoma. J Clin Oncol 2004;22:133–42.

21. Arteaga CL. Epidermal growth factor receptor dependence in human tumors: more than just expression? Oncologist 2002;4:31–9.

22. Normanno N, Bianco C, De Luca A, Salomon DS. The role of EGF-related peptides in tumor growth. Front Biosci 2001;6:D685–707.

23. Phillips AC, Ernst MK, Bates S, Rice NR, Vousden KH. E2F-1 potentiates cell death by blocking antiapoptotic signaling pathways. Mol Cell 1999;4:771–81.

24. Sherr CJ. Tumor surveillance via the ARF-p53 pathway. Genes Dev 1998;12: 2984–91.

25. Furukawa Y, Nishimura N, Satoh M, et al. Apaf-1 is a mediator of E2F-1-induced apoptosis. J Biol Chem 2002;277:39760–8.

26. Mannick JB, Hausladen A, Liu L, et al. Fas-induced caspase denitrosylation. Science 1999;284:651–4.

27. Hueber AO. CD95: more than just a death factor? Nat Cell Biol 2000;2: E23–5.

28. Chen F, Castranova V, Shi X, Demers LM. New insights into the role of nuclear factor-κB, a ubiquitous transcription factor in the initiation of diseases. Clin Chem 1999;45:7–17.

29. Ryan KM, Ernst MK, Rice NR, Vousden KH. Role of NF-κB in p53-mediated programmed cell death. Nature 2000;404:892–7.

30. Hoffmann A, Levchenko A, Scott ML, Baltimore D. The IκB-NF-κB signaling module: temporal control and selective gene activation. Science 2002; 298:1241–5.

31. Pao W, Wang TY, Riely GJ, et al. KRAS mutations and primary resistance of lung adenocarcinomas to gefitinib or erlotinib. PLoS Med 2005; 2:e17.

32. Lu C, Speers C, Zhang Y, et al. Effect of epidermal growth factor receptor inhibitor on development of estrogen receptor-negative mammary tumors. J Natl Cancer Inst 2003;95:1825–33.

33. Chaparro J, Reeds DN, Wen W, et al. Alterations in thigh subcutaneous adipose tissue gene expression in protease inhibitor-based highly active antiretroviral therapy. Metabolism 2005;54:561–7.

34. Dahlquist KD, Salomonis N, Vranizan K, Lawlor SC, Conklin BR. GenMAPP, a new tool for viewing and analyzing microarray data on biological pathways. Nat Genet 2002;31:19–20.

Molecular Cancer Research

Effect of an Epidermal Growth Factor Receptor Inhibitor in Mouse Models of Lung Cancer

Ying Yan, Yan Lu, Min Wang, et al.

Mol Cancer Res 2006;4:971-981.